Navas *et al. Bioresour. Bioprocess.* (2020) 7:4
https://doi.org/10.1186/s40643-019-0291-3

Bioresources and Bioprocessing

RESEARCH Open Access

A sustainable process for biodiesel production using Zn/Mg oxidic species as active, selective and reusable heterogeneous catalysts

Marisa B. Navas, José F. Ruggera, Ileana D. Lick and Mónica L. Casella*

Abstract

This paper describes the preparation and characterization of MgO and ZnO-based catalysts, pure and mixed in different proportions, supported on γ-Al_2O_3. Their catalytic performance was studied in the transesterification of soybean oil and castor oil with methanol and butanol, attempting to produce biodiesel. XRD (X-ray diffraction), SEM–EDS (scanning electron microscopy–energy dispersive X-ray spectroscopy), CO_2-adsorption and N_2-adsorption allowed characterizing the prepared catalysts. The characterization results were in all cases consistent with mesoporous solids with high specific surface area. All the catalysts exhibited good results, especially in the transesterification of castor oil using butanol. For this reaction, the reuse was tested, maintaining high FABE (fatty acid butyl esters) yields after four cycles. This good performance can be attributed to the basic properties of the Mg species, and simultaneously, to the amphoteric properties of ZnO, which allow both triglycerides and free fatty acids to be converted into esters. Using these catalysts, it is possible to obtain second-generation biodiesel, employing castor oil, a raw material that does not compete with the food industry. In addition, butanol can be produced from renewable biomass.

Keywords: Biodiesel, Heterogeneous catalysts, Soybean oil, Castor oil, Transesterification, Mg/Zn species

Introduction

The growing demands of energy in sectors such as transport or various industries, require the need for replacement of non-renewable fossil fuels. Renewable fuels appear as an attractive option to satisfy this demand. Nowadays, there is a classification for these biofuels, which include: first generation, those produced from highly available food sources; second generation, those generated using non-edible raw materials or involving advanced technologies; third generation, including biofuels from algae; and finally, fourth generation, those including biofuels produced from genetically modified algae (Hoekman et al. 2012; Abdullah et al. 2019).

Biodiesel attracted much attention as alternative energy source, since it is renewable, sustainable and biodegradable. In addition, biodiesel presents a lower emission of particulate matter and NOx. These environmental benefits are due to the absence of sulfur compounds and aromatic residues in the oils (Alaei et al. 2018; Shan et al. 2018). Biodiesel not only has environmental advantages, but also has properties that make it a good fuel, such as its high ignition point, excellent lubricity and miscibility with petroleum fuels, what allows it to produce different blends (Knothe and Razón 2017). Nowadays, biodiesel can be produced in a cleaner and less expensive way, using advanced technologies and waste sources, like biowaste oil (Chuah et al. 2017).

*Correspondence: casella@quimica.unlp.edu.ar
Centro de Investigación y Desarrollo en Ciencias Aplicadas "Dr. Jorge J. Ronco" (CINDECA) (CCT-La Plata CONICET, UNLP, CICPBA), Departamento de Química, Facultad de Ciencias Exactas, Universidad Nacional de La Plata, Calle 47 No 257, 1900 La Plata, Argentina

Biodiesel is defined as a mixture of alkyl esters of long-chain fatty acids. For the production at an industrial level, generally short-chain alcohols (methanol, ethanol or butanol) are used in the transesterification of vegetable oils or animal fats (Lin et al. 2006). The transesterification reaction involves three consecutive and reversible steps. At each step, an alkyl ester of a fatty acid molecule is generated for each molecule of alcohol consumed. Triglycerides are converted into diglycerides and monoglycerides, and finally into glycerol, the main byproduct (Issariyakul and Dalai 2014). Biodiesel can be also produced through the esterification of the free fatty acids (FFA) present in the raw material (da Silva Filho et al. 2018).

Vegetable oils are the most chosen source of triglycerides in biodiesel production. The climatic, socio-economic and cultural conditions are fundamental in the choice of the oil. The characteristic crops of each region are the essential source for obtaining these oils. For example, in Argentina and Brazil soybean, canola or sunflower oil are used, in India, on the other hand, jatropha oil is mostly used (Ullah et al. 2016). Vegetable oils are chosen over animal fats due to their renewability, biodegradability and lower content of aromatic compounds and sulfides, producing biodiesel in a less harmful way to the environment (Koh and Mohd Ghazi 2011). Furthermore, considering the world demand for food, biodiesel can be produced using vegetable oils that do not compete with food industry. This is called, as mentioned previously, second-generation biodiesel. The biodiesel production from non-edible raw materials is a field that is being extensively explored, so it is necessary to develop studies on different sources of triglycerides that do not compete with the food industry. Selecting these types of vegetable sources allows, in turn, to reduce biodiesel production costs (Zhang et al. 2018a). Among the options already known and studied are *Jatropha curcas* crude oil, *Silybum marianum* oil, *Firmiana platanifolia* L.f. oil and *Euphorbia lathyris* crude oil (Adeniyi et al. 2019; Zhang et al. 2018b, Pan et al. 2018). Castor oil is an excellent alternative (Elango et al. 2019). This oil is mainly composed of the ester derived from the ricinoleic acid (9Z, 12R)-12-hydroxy-9-octadecenoic acid). Also, castor seeds have greater potential over other crops, since it contains 40–55 wt% of oil. The soybean oil contains 15–20% of oil, for example (Keera et al. 2018). It has been demonstrated that the presence of hydroxyl group in the ricinoleic acid favors both the synthesis and the use of the derived biodiesel (Wang and Sun 2016). Due to this particular chemical composition, castor oil presents higher viscosity and polarity than other oils, what allows its employment in various industries (Conceição et al. 2007).

Transesterification is generally carried out using methanol or ethanol as reagents, both good fatty acid acyl acceptors (Sun et al. 2019). On the contrary, butanol has not been so extensively investigated. This alcohol presents a higher boiling point in comparison with other short-chain alcohols; it is also less corrosive and less soluble in water, and consequently has a greater miscibility with the oil phase (Steen et al. 2008). The use of butanol over other short-chain alcohols, such as methanol or ethanol, would be preferred, since its longer chain favors the properties of the final biodiesel, as well as its blending with conventional diesel. Besides, the butyl ester has a higher energy value than the analogues methyl or ethyl esters, since it contains more carbon atoms. Moreover, butyl ester has a higher cloud point than methyl esters (Hájek et al. 2017). In addition, butanol also has the advantage of being produced from different types of renewable sources. Then, bio-butanol can be produced by fermentation of lignocellulosic materials (agricultural or paper waste, for example), or non-cellulosic materials (corn or molasses, for example) (Kumar and Gayen 2011; Kolesinska et al. 2019). Given the properties of butanol for biodiesel production, more research is needed in this regard.

The biodiesel production can be carried out using homogeneous and heterogeneous catalysis. Nevertheless, the use of homogeneous catalysts favors the formation of unwanted soaps, which is a disadvantage in the separation and purification steps of the process (Margellou et al. 2018). In this sense, heterogeneous catalysis is more convenient, mainly thanks to an easier separation of the catalyst from the reaction products. This allows the catalysts to be washed and reused. In addition, heterogeneous catalysis does not produce soaps (Boonyuen et al. 2018). Nevertheless, the presence of FFA can generate soaps, which is why more efficient catalysts have to be studied, and these systems must be optimized. An example of this is the work developed by Sun et al. (Sun and Li 2016). The basic catalysts are preferred, since they allow using mild reaction conditions. Catalysts with a good performance have been reported, including supported metal oxides and hydrotalcites (Lee and Wilson 2015).

MgO has been used as a transesterification catalyst, although it presents limitations regarding its weak basic strength and solubility (Sharma et al. 2011). To improve its catalytic performance, a possible alternative is to generate a binary system with another species like other metal oxides. It is known from the literature that the addition of ZnO can enhance the activity of MgO, given its amphoteric properties (Veiga et al. 2016).

In this work, in order to develop a more sustainable process, the transesterification of soybean oil and castor oil, using methanol and butanol has been investigated. Different mixtures of Mg and Zn oxidic species were developed as catalysts. Castor oil was chosen because it

is a non-edible raw material, aiming to solve the issue of competition with the food industry. Therefore, it allows obtaining second-generation biodiesel. Given the superior properties of biodiesel prepared from butanol, instead of methanol or ethanol, butanol was selected for the transesterification reaction. It is important to highlight that butanol can also be obtained from renewable sources, since bio-butanol can be obtained by fermentation, generating a sustainable process to produce biodiesel. The combination of two renewable, environmentally friendly raw materials that improve the biodiesel properties, is an important step oriented to the production of second-generation biodiesel.

Materials and methods

Catalyst preparation

Mg and Zn catalysts, pure and mixed in different proportions, were prepared by the conventional method of coprecipitation of carbonates, followed by calcination [Lee et al. 2013]. The precursors were supported on γ-Al_2O_3, meshed and sieved to 60–100 mesh. The total amount of supported oxides was 0.17 mol (MgO + ZnO) per 100 g of alumina. Mg/Zn mixtures were prepared with Zn/Mg atomic ratios of 0.5, 1.0, 1.5 and 2.0.

In a typical preparation, the necessary amount of Mg and Zn nitrates (supplied by Biopack and Anedra) were dissolved in an aqueous suspension of γ-Al_2O_3. Then, $(NH_4)_2CO_3$ 1 M was added under vigorous stirring. The pH was controlled at a value of 9, using NH_4OH. The solution was stirred for 2 h, aged, and then the solid was filtered and dried at 60 °C overnight. The active phases were obtained after calcination at 500 °C.

Catalyst characterization

The elemental composition of the catalysts was determined by atomic absorption spectroscopy using a Varian 240 equipment. For each sample, the digestion was carried out using concentrated HCl on hot plate. The lines employed were 202.6 nm for Mg lamp, and 213.9 nm for Zn lamp.

The textural properties of the different catalysts were determined by N_2 physisorption at − 196 °C, employing a Micromeritics ASAP 2020 analyzer, and the total surface area (S_{BET}) was calculated by the BET (Brunauer–Emmett–Teller) method.

The crystalline phases present were determined using an X-ray diffractometer Philips PW 1740 (Cu Kα radiation, λ = 0.154 nm). The samples were scanned from 5° to 75° at the scanning speed of 1 min^{-1}.

In order to study the basicity of the prepared catalysts, the amount of adsorbed CO_2 was quantified by thermogravimetric analysis, using a Shimadzu TGA-50 equipment. The analysis conditions are detailed in Navas et al. 2018.

Scanning electron microscopy images were obtained with a Philips Scanning Electron Microscope 505. The energy dispersive X-ray analysis (EDS) was performed using an EDAX DX PRIME 10 analyzer at a working potential of 15 kV. To establish the dispersion of the active species on the catalysts, a qualitative mapping of the surface was performed.

FTIR spectra of both the fresh and post-reaction 0.5 Zn/Mg catalyst were recorded in the diffuse reflectance mode on a Thermo Avatar 360 instrument, using a DTGS detector. The spectra were averaged from 120 scans in the range of 400–4000 cm^{-1} at a resolution of 4 cm^{-1}. To detect the probable presence of carbonaceous deposits on the post-reaction catalyst, oxidation thermogravimetric analysis was performed using a thermobalance (Shimadzu TGA-50) with a heating rate of 10 °C/min and an air/He feed (2:1). For both the fresh and post-reaction catalyst, the mass used was 10 mg. The weight loss and the temperature were recorded as a function of time. The derivative curve (DTGA) was obtained from the weight loss information as a function of time.

Transesterification procedure

The catalysts performance was studied in the transesterification reaction, employing two vegetable oils, soybean oil and castor oil (one at a time, without mixtures between them) and two alcohols, methanol (Cicarelli, 99.8%) and butanol (Merck, 99.4%) (again, one at a time). In order to differentiate the studied oils, in terms of their characteristics, their compositions are presented in Table 1.

The reaction was conducted in a 250-cm^3 three-necked batch glass reactor, provided with a reflux condenser reflux and a mechanical stirrer. Alcohol/oil molar ratio,

Table 1 Typical fatty acid composition (%) of soybean oil and castor oil (Meneghetti et al. 2006, 2007)

Fatty acid	Fatty acid content (%)	
	Soybean oil	Castor oil
Myristic (14:0)	0.2	–
Palmitic (16:0)	16.0	1.8
Stearic (18:0)	2.4	–
Oleic (18:1)	23.5	–
Linoleic (18:2)	51.2	11.2
Linolenic (18:3)	8.5	–
Ricinoleic (18:0(OH))	–	87.0
Total C18	85.6	98.2
Free fatty acids (FFA)	0.1	1.2

catalyst amount and reaction temperature were established at 6:1; 5 wt%, and 60 °C for methanol and 80 °C for butanol (Navas et al. 2018). These values were determined from a previous optimization study on the soybean–methanol oil system carried out by our research group (Sánchez et al. 2014).

The product analysis was carried out by a GC (gas chromatography) method according to EN (European Standard) 14105 and ASTM (American Society of Testing Materials) D6584 [EN 14105; ASTM D6584], using a GC-2010 Plus Tracera Gas Chromatograph, equipped with a BID detector. A MEGA-Biodiesel 105 (15 m × 0.32 mm × 0.10 μm) capillary column was used. Samples were taken after 2, 4 and 6 h of reaction, except other specified. The pre-injection treatment of the samples, as well as the chromatographic conditions, is detailed in Navas et al. 2018. This previous work also specified the equations used for the calculation of triglyceride conversion, selectivity to monoglycerides or diglycerides, and FAME (fatty acid methyl ester) or FABE yield and selectivity (Navas et al. 2018).

Results and discussion

Catalyst characterization

The elemental composition of the catalysts was determined by AAS (atomic absorption spectroscopy). Table 2 gathers these results, and the nominal contents of the oxides have also been included. As can be observed, the experimental atomic ratio was quite similar to the theoretical one, for all the studied catalysts, except for the 2 Zn/Mg catalyst in which the zinc content is substantially lower than expected. The difference found may be accounted for the pH control in the preparation, since MgO and ZnO require different pH values for an optimal precipitation (Ngamcharussrivichai et al. 2008; Lee et al. 2011).

Table 2 also presents the textural properties of different catalysts, determined by N_2 physisorption. For all the catalysts, the pore distribution showed the presence of macro and mesoporous. The mesopore diameters for the Zn/Mg catalysts were slightly higher than for the pure oxide catalysts. Observing the macropore values, ZnO/γ-Al_2O_3 catalyst presented a value of 67 Å, a considerably higher value than that observed for MgO/γ-Al_2O_3 catalyst and the Zn/Mg mixtures, that range between 52 and 57 Å. The pore distribution graphs can be found as Additional file 1.

For 0.5 Zn/Mg and 2 Zn/Mg catalysts, the specific surface area decreases with respect to the pure γ-Al_2O_3. This result is a sign of the existence of an interaction between both metals with the support. It is worth noting that the catalyst with the Zn/Mg atomic ratio of 1.5 has the highest specific surface and also shows a slight decrease in the pore volume, which could indicate the presence of some segregated phase on the surface. On the other hand, the 2 Zn/Mg catalyst presented a S_{BET} value quite similar to that of the ZnO/γ-Al_2O_3 catalyst, maybe due to its high Zn proportion. The synthesis method used in this work allows obtaining catalysts whit high specific surface areas. Olutoye and Hameed have studied mixed Mg and Zn supported oxides, using $Al(NO_3)_3$ as a precursor instead of commercial Al_2O_3 and found that this method led to the formation of mixed phases with surfaces around 50 $m^2\ g^{-1}$, while in this work values of between 150 and 250 $m^2\ g^{-1}$ have been obtained (Olutoye and Hameed 2013). Considering that these solids will be used in a heterogeneous process, a high surface area is a desirable property.

Figure 1 depicts the obtained isotherms, which are type IV for all catalysts, attributed to macro and mesoporous materials (Thommes et al. 2015). The isotherms of the mixed oxides are more similar to MgO/γ-Al_2O_3 (Fig. 1,

Table 2 Textural properties and chemical composition of the prepared catalysts

Catalyst	S_{BET} (m^2/g)	V_{pore} (cm^3/g)	d_{pore} (Å)		MgO (wt%)[a]	MgO (wt%)[b]	ZnO (wt%)[a]	ZnO (wt%)[b]	Zn/Mg[c]	Zn/Mg[d]
			Mesopores	Macropores						
MgO/γ-Al_2O_3	223	0.43	32	57	6.85	nd	–	–	–	–
0.5 Zn/Mg	168	0.32	36	57	4.67	4.14	4.61	5.72	0.5	0.68
1 Zn/Mg	232	0.35	37	51	3.42	3.81	6.26	5.47	1.0	0.71
1.5 Zn/Mg	266	0.41	37	52	2.74	3.15	8.30	9.21	1.5	1.45
2 Zn/Mg	182	0.39	37	51	2.28	1.82	9.22	6.22	2.0	1.69
ZnO/γ-Al_2O_3	173	0.42	32	67	–	–	13.83	nd	–	–
γ-Al_2O_3	216	0.45	nd	75	–	–	–	–	–	–

[a] Nominal value

[b] Measured by AAS

[c] Theoretical atomic ratio

[d] Experimental atomic ratio (through AAS measurements)

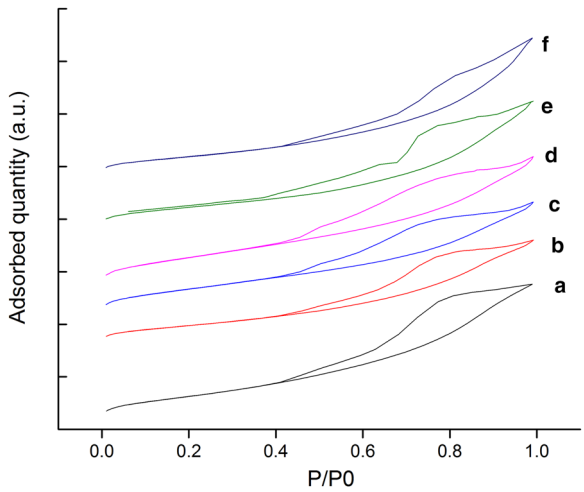

Fig. 1 BET isotherms for the prepared catalysts: (a) MgO/γ-Al_2O_3; (b) 0.5 Zn/Mg; (c) 1 Zn/Mg; (d) 1.5 Zn/Mg; (e) 2 Zn/Mg and (f) ZnO/γ-Al_2O_3

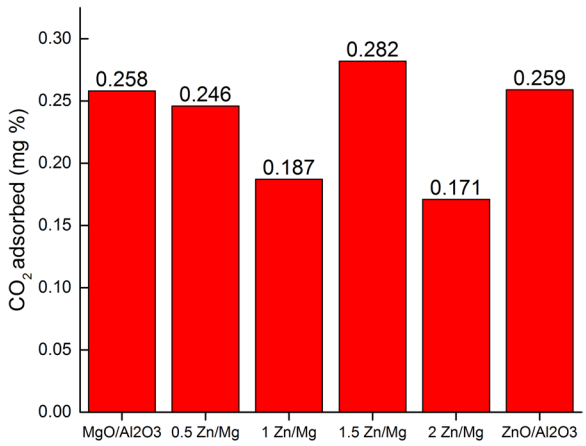

Fig. 2 Results of CO_2 adsorption for the prepared catalysts

curve a) than to ZnO/γ-Al_2O_3 (Fig. 1, curve f). All the desorption branches indicate percolation of pores, especially in 2 Zn/Mg catalyst, where the percolation evidently occurs in two different types of pores, due to the observed irregularity. Hysteresis loops for the isotherms of all studied catalysts correspond to H2 type, according to IUPAC classification (Thommes et al. 2015). H2 type loop is broad with a long and almost flat plateau and a steep desorption branch. Many inorganic oxides give the more common type H2 loops. The pore structures in these materials are generally complex and tend to be made up of interconnected networks of pores of different size and shape (Neimark et al. 2008).

To estimate the basicity of the catalysts, CO_2 adsorption tests were carried out. The obtained results, presented in Fig. 2, are expressed as mg of CO_2 adsorbed per 100 mg of catalyst. The 1.5 Zn/Mg catalyst exhibited the highest value of CO_2 adsorption (0.282 mg%), this result being even higher than those of MgO/γ-Al_2O_3 and ZnO/γ-Al_2O_3 (0.258 mg% and 0.259 mg%, respectively). It is possible to infer that the 1.5 Zn/Mg catalyst has higher density of basic sites than the monometallic catalysts and probably this fact can be associated with a higher exposure of the active sites because of the higher surface area presented by this catalyst. The 0.5 Zn/Mg catalyst presented a slightly lower value than the monometallic catalysts. On the other hand, 1 Zn/Mg and 2 Zn/Mg catalysts presented values considerably smaller than those samples. It can be considered that, despite the small differences observed, the amount of CO_2 adsorbed is similar for all the catalysts, indicating the presence of basic sites in all of them, even in the ZnO/γ-Al_2O_3 catalyst. This similarity could be associated to the presence of basic sites of the MgO, as well as to a certain adsorption capacity of the alumina, which, being the support, is found in the highest proportion in all the catalysts.

The XRD patterns obtained are shown in Fig. 3. In every pattern, the broad peaks corresponding to the presence of a transition alumina phase, located at 37.6°, 45.8° and 66.8° (JCPDS (Joint Committee on Powder Diffraction Standards) card no 29-1480) can be observed. It was not possible to identify peaks of MgO phase in the MgO/γ-Al_2O_3 catalyst, even though Mg has been measured by atomic absorption (Table 2). This could be due to the fact that the crystals are too small to be detected by XRD technique. The MgO phase was neither

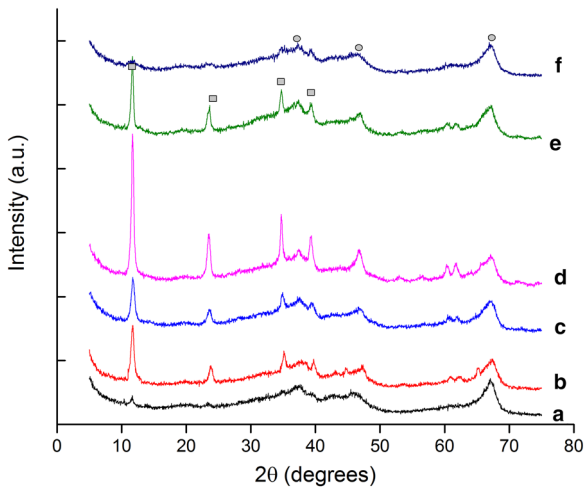

Fig. 3 XRD patterns for the prepared catalysts. (a) MgO/γ-Al_2O_3; (b) 0.5 Zn/Mg; (c) 1 Zn/Mg; (d) 1.5 Zn/Mg; (e) 2 Zn/Mg and (f) ZnO/γ-Al_2O_3

observed in the Mg nor Zn-containing catalysts. In the zinc-containing catalysts, no diffraction lines associated with the presence of crystalline phases of ZnO, either of hydroxides or of Zn aluminium oxide were observed. The ZnO/γ-Al_2O_3 catalyst, despite having the highest concentration of Zn, did not exhibit peaks corresponding to the zincite phase (JCPDS no 22-1034). However, in the diffractograms of the Zn-containing catalysts very intense signals located at $2\theta = 11.77°$; 23.3°; 34.8°; 46.8°, 60.56° and 62.09° appear, which can be associated with the presence of mixed aluminium and magnesium oxidic phases, such as magnesium aluminium hydroxide (PDF 00-0351275) or magnesium aluminium hydroxide hydrate (PDF 00-0350965). It should be noted that both 1.5 Zn/Mg and 2 Zn/Mg catalysts, which contain the highest zinc content, the diffraction lines corresponding to the magnesium aluminium hydroxide crystalline phase are more intense and narrower, indicating an increase in the crystallinity of the segregated phase. It is evident that the addition of zinc modifies the characteristics of the magnesium phases, segregating hydrated phases that modify the surface properties of the catalysts, its capacity to absorb CO_2 among others.

The images obtained by SEM are presented in Fig. 4. Monometallic catalysts showed porous surfaces with small particles, exhibiting different morphologies: the MgO particles have small filaments on their surface, while ZnO particles are small sheets with appearance of "flakes". The images of the Zn/Mg catalysts showed that those with a higher proportion of MgO have a morphology similar to MgO, with small and thin filaments on the surface; and those with a higher proportion of ZnO exhibit the small "flakes". In the surface of 1.5 Zn/Mg catalyst, the small particles appear to be melted together. To investigate about the distribution of the different species on the surface of the catalysts, EDS analysis and a qualitative mapping of Mg and Zn was carried out. Figure 5 shows the result of the mapping for the 0.5 Zn/Mg catalyst and, as can be seen, both elements have a homogeneous dispersion on the alumina surface. Regarding the Zn/Mg ratio measured by this technique, the results were quite similar to those obtained by AAS for all the catalysts.

Catalytic activity

Transesterification of soybean oil using methanol

Initially, catalysts were used in the classical transesterification reaction of soybean oil with methanol. The selectivities and FAME yield obtained are presented in Fig. 6. The results show that the addition of Zn does not favor the transesterification of soybean oil with methanol, as the FAME yield decreases progressively by increasing the Zn proportion. The addition of Zn modifies the basic properties of the catalyst, due to its amphoteric behavior. This makes the catalysts less active in the transesterification. The widely accepted mechanism for

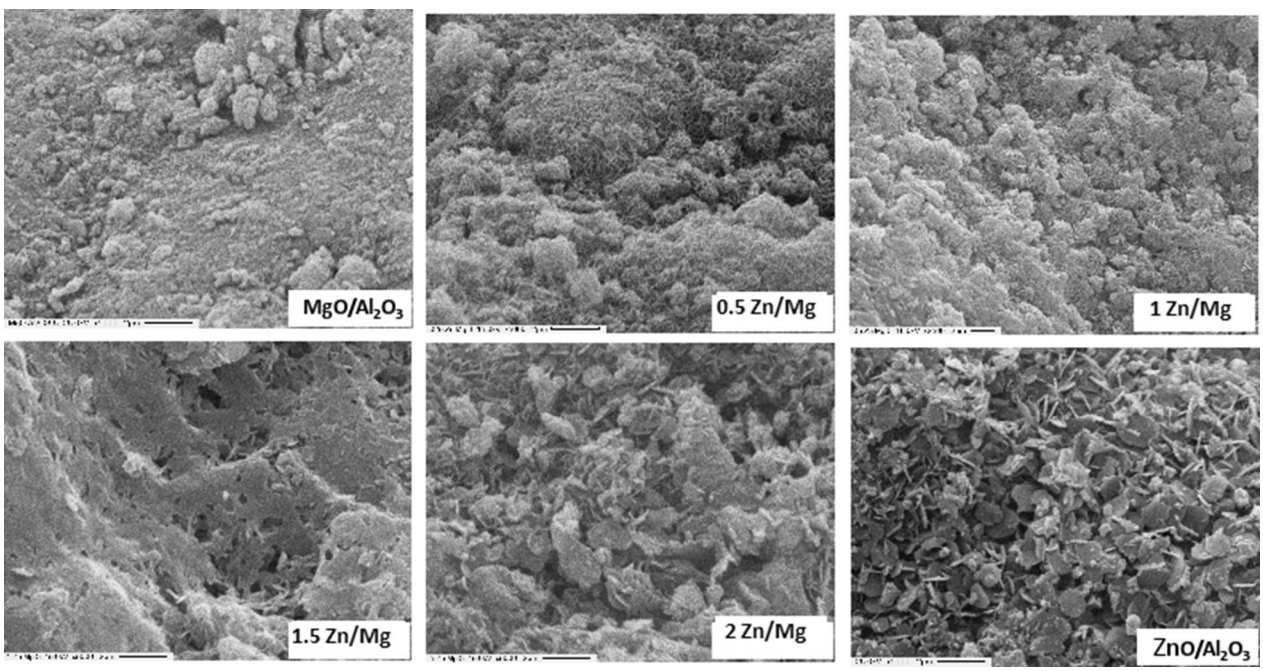

Fig. 4 SEM images for catalysts

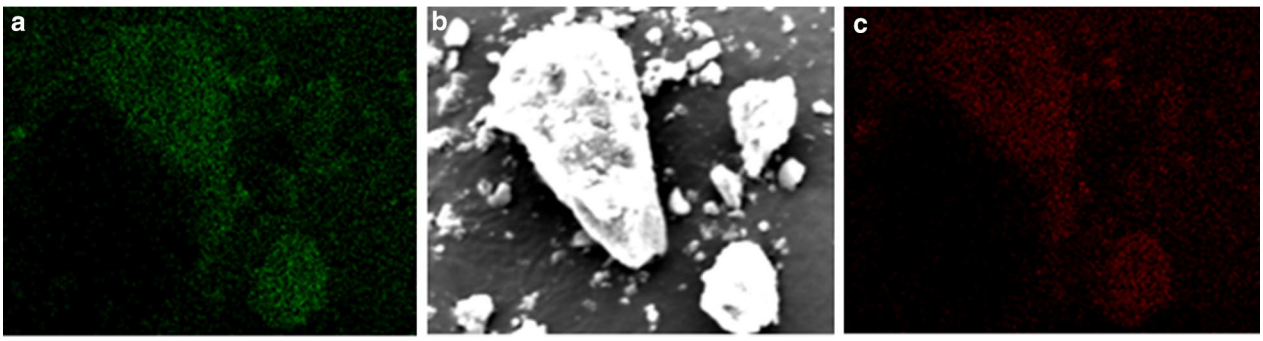

Fig. 5 Qualitative mapping of 0.5 Zn/Mg surface. **a** Mg mapping; **b** SEM image (×200); **c** Zn mapping

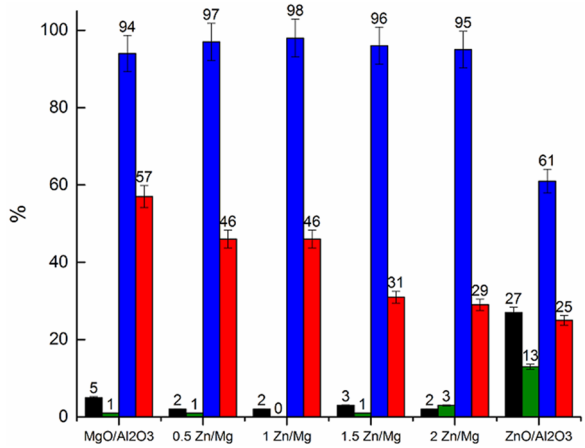

Fig. 6 Selectivity to monoglycerides (black square), diglycerides (green square) and FAME (blue square), and FAME yield (red square) obtained for each catalyst, in the transesterification of soybean oil with methanol

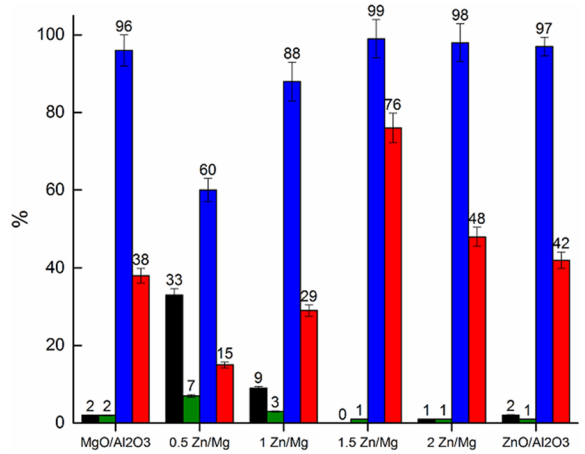

Fig. 7 Selectivity to monoglycerides (black square), diglycerides (green square) and FAME (blue square), and FAME yield (red square) obtained for each catalyst, in the transesterification of castor oil with methanol

transesterification reaction by basic heterogeneous catalysis, initially comprises the formation of the methoxide anion and an alkoxycarbonyl intermediary, on basic sites on the surface (Pasupulety et al. 2015; Navas et al. 2018). The presence of Zn modifies the nature of the active sites, disfavouring the yield of FAME.

These results are in accordance to those found by Lee et al., who reported the study of mixtures of Mg and Zn oxides, in which the catalytic activity grows as the basicity increases (Lee et al. 2013). Lee et al. prepared mass catalysts; exhibiting BET surface values around 10 $m^2\ g^{-1}$. In this work, the applied catalysts present the advantage of exhibiting much larger surfaces, due to the use of γ-Al_2O_3 as support, what would contribute to the catalytic performance.

Using the mixed oxides, the FAME selectivity improved notably in relation to ZnO/γ-Al_2O_3 (61%). The FAME selectivity to FAME exceeded 95% for the rest of the catalysts tested, also improving the FAME selectivity exhibited using MgO/γ-Al_2O_3 (94%). Therefore, using a mixture of Mg and Zn oxides, even in a minimal proportion of Zn, allows the transesterification reaction to proceed more selectively to FAME.

Transesterification of castor oil using methanol

As a contribution to the development of a more sustainable process, a non-edible oil was selected as reactive. To do so, castor oil was employed instead of castor oil. The results of the transesterification employing methanol are presented in Fig. 7.

All the catalysts showed good FAME selectivity, except for 0.5 Zn/Mg, which only reached 60%. The FAME selectivity is increased by adding Zn, until it reaches the 1.5 Zn/Mg ratio, and then it remains approximately constant. The 0.5 Zn/Mg catalyst presented the lowest

performance in the series (15%); this can be attributed to the low specific surface between all Zn/Mg catalysts.

In general, Zn/Mg catalysts produced better yields using an oil with a higher amount of free fatty acids (FFA). MgO provides the necessary basicity to carry out transesterification, while ZnO favors the esterification of FFA, due to its amphoteric properties (Yan et al. 2009).

1.5 Zn/Mg catalyst presented the highest FAME yield (76%), and a high FAME selectivity (99%), so it can be considered as the best of the series in the transesterification of castor oil and methanol. This same catalyst did not show a good performance in the analogous reaction with soybean oil (31%). Then, 1.5 Zn/Mg appears to be a more efficient catalyst in the transesterification of oils of lower quality, due to the amphoteric properties of ZnO. Castor oil contains a greater amount of free fatty acids (FFA) than soybean oil (Table 1), which can be esterified.

Transesterification of soybean oil using butanol

The Zn/Mg catalysts were further evaluated in the transesterification of soybean oil using butanol, an alcohol that can be obtained from biomass. Figure 8 presents the different selectivities and the performance to FABE for each catalyst. It is remarkable that all catalysts showed FABE selectivities very close to 100%. The catalyst 1.5 Zn/Mg presented the highest FABE yield (66%), which was also the only one that exceeded the percentages exhibited by MgO/γ-Al_2O_3 and ZnO/γ-Al_2O_3 (50% and 42%, respectively).

In general, the addition of ZnO increases the catalytic activity for transesterification between soybean oil and butanol, except for 2 Zn/Mg catalyst. Using this catalyst, FABE yield decreases to a large extent. This may be due to the ZnO ratio is too high to allow transesterification of the soybean oil, a reagent without a significant proportion of FFA. Also, the specific surface increases as the amount of ZnO increases, except for 2 Zn/Mg catalyst. The same is observed for the FABE yields obtained. Then, for this mixture of reagents, the specific surface is a factor to be taken into account.

It is notorious that the reaction using 2 Zn/Mg catalyst reached lower FABE yield than the reaction using ZnO/γ-Al_2O_3, even when the catalysts exhibits similar specific surfaces. This could be due to the low proportion of MgO in the catalyst, which would notably decrease the density of basic sites, and therefore, the catalytic activity (Lee et al. 2013). Also, the SEM micrographs obtained for this catalyst presented only large flake-like particles belonging to ZnO.

Transesterification of castor oil using butanol

Finally, the prepared catalysts were evaluated in the transesterification of castor oil, using butanol. The obtained percentages of FABE yield are presented in Fig. 9. All catalysts reached FABE selectivity of approximately 100%. This means that the conversion of triglycerides is complete, and also directed towards the esters, the desired reaction product. The prepared catalysts resulted exceptionally active in the transesterification between these reagents. The catalytic activity is favored for the considerably values of specific surface exhibited by the catalysts, which exposes a great number of pores. In these pores, the active sites for the reaction are located.

Besides, the mixture of MgO and ZnO allows producing simultaneously the transesterification of triglycerides and the esterification of free fatty acids (FFA). Castor

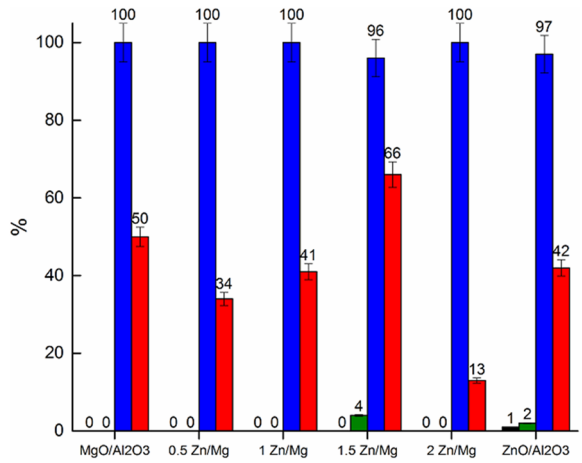

Fig. 8 Selectivity to monoglycerides (black square), diglycerides (green square) and FAME (blue square), and FAME yield (red square) obtained for each catalyst, in the transesterification of soybean oil with butanol

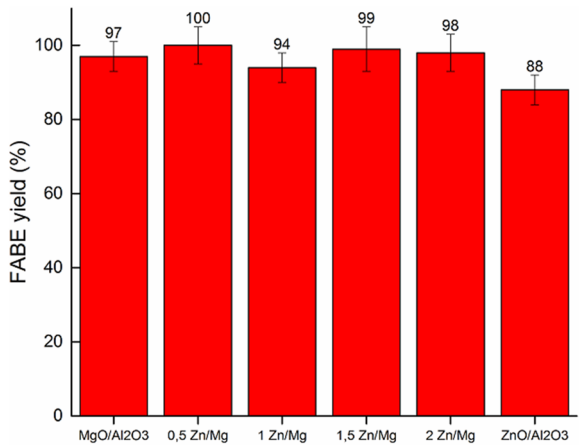

Fig. 9 FABE yield (%) obtained for the prepared catalyst, in the transesterification of castor oil with butanol

oil is considered a "low-quality oil", due to its content of approximately 1.2% of FFA (Table 1), susceptible of being esterified. ZnO, thanks to its amphoteric properties, promotes both transesterification and esterification (Yan et al. 2011).

FABE yield (%) was evaluated more in detail for 0.5 Zn/Mg, due to the good result obtained with this catalyst. FABE yield obtained after each hour of reaction is presented in Fig. 10. The reaction present good yields of FABE even after 1 h of reaction (95%), and the maximum yield is reached at 3 h of reaction.

The advantage of using a catalyst of this type lies in the fact that both transesterification and esterification reactions can be carried out in a single step. Generally, oils with a high FFA content require an initial stage that allows them to be removed or converted into esters, to then perform transesterification, avoiding the saponification reaction (Borges and Díaz 2012).

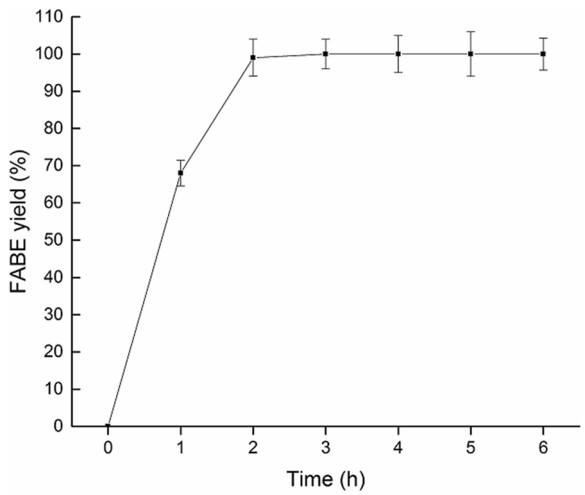

Fig. 10 FABE yield (%) obtained in the transesterification between castor oil and butanol, using 0.5 Zn/Mg

Castor oil presented a higher solubility in butanol, than in methanol or ethanol. This high miscibility is extremely favorable for the reaction and contributes to the interaction between the reagents (Baskar and Soumiya 2016; Keera et al. 2018).

These results are encouraging; facing the production of second-generation biodiesel, because castor oil is a non-edible raw material. Moreover, butanol is an attractive option, feasible to be produced from biomass, a renewable source.

Table 3 presents a comparison of our results and different recently optimized catalytic systems, using different alcohols and vegetable oils in the transesterification reaction. The FABE yields obtained in our work, specifically for the mixture castor oil–butanol are very good. These results were achieved using an amount of catalyst lower than that presented in the considered systems. Besides, the alcohol:oil ratio employed is also lower than other transesterification reactions. This indicates that, for the transesterification of castor oil using butanol, and employing the prepared Mg/Zn catalysts, excellent FABE yields can be obtained using a minimum excess of alcohol over the stoichiometric ratio.

It is worth mention that the same reaction conditions optimized in a previous work for the soybean–methanol oil system were used the present paper (Sánchez et al. 2014), obtaining even better results.

Table 3 Comparison of results between different catalytic systems

	Catalyst	Oil	Alcohol	Conditions			Selectivity to esters (%)	Yield of esters (%)	Conversion (%)
				Alcohol:oil ratio	%wt catalyst	Temperature (°C)			
This work	1.5 Zn/Mg-γAl_2O_3	Castor oil	Butanol	6:1	5	80	> 99	> 99	> 99
Mahdavi and Monajemi (2014)	CaO-MgO/Al_2O_3	Cottonseed oil	Ethanol	8.5:1	14.4	95	–	–	97.6
Chuayplod and Trakarnpruk (2009)	Mg(Al)La hydrotalcites	Rice bran oil	Methanol	30:1	7.5	75	97	78	–
Rahman et al. (2019)	Zn–CaO	Eucalyptus oil	Methanol	6:1	5	65	–	93.2	–
Rubio-Caballero et al. (2009)	$CaZn_2(OH)_6{\cdot}2H_2O$	Sunflower oil	Methanol	12:1	4	60	–	> 90	–

Catalyst recycling

An important aspect of a heterogeneous catalyst is its stability and the possibility of being reused. After the transesterification of castor oil with butanol, 0.5 Zn/Mg catalyst was removed; then washed with methanol on a hot plate to eliminate any oil residue adhered to the surface. The catalyst was finally dried overnight and calcined 2 h at 500 °C, in order to burn any organic deposit and regenerate the active sites in the surface.

The 0.5 Zn/Mg catalyst was reused in the transesterification of castor oil using butanol. The results obtained are presented in Fig. 11. It is observed that after an initial decrease in the catalytic performance between the first and second catalytic runs, from then on, the obtained yield remains approximately constant. The catalyst continued to generate acceptable results, preserving a 100% FABE selectivity.

In order to obtain chemical information about the post-reaction catalyst, XRD, FTIR and thermogravimetric analysis were carried out. The results obtained are presented in Fig. 12a–c, respectively. Slight changes in the physicochemical properties of the catalyst were observed. Figure 12a shows the diffractograms obtained for the catalyst before and after its use in the reaction. The crystalline phases initially detected remain after 4 recycling cycles. However, a higher degree of crystallinity is observed in the regenerated sample, since the already mentioned peaks at $2\theta = 11.77°$; 23.3°; 34.8°; 46.8°, 60.56° and 62.09° are sharper and more intense in this sample.

Figure 12b exhibits the DRIFT spectra for the fresh 0.5 Zn/Mg catalyst and the same catalyst after 4 reaction cycles. No substantial differences between both spectra can be observed, evidencing that there are not any adsorbed species remaining on the surface. In both spectra, a broad band between 2700 and 3800 cm^{-1} can be identified, due to the stretching of the surface hydroxyl groups. This band is usually found in materials such as MgO, ZnO and Al_2O_3 (Xi and Davis 2011). The bands observed in the region between 1250 and 1800 cm^{-1} can be assigned to the symmetric and antisymmetric water bending (Bagabas et al. 2013). In the region below 1000 cm^{-1}, a broad band can be observed, corresponding to the overlapping of the absorption bands assigned to the stretching of Al-O (ca. 560, 788 and 940 cm^{-1}), Mg–O (645 cm^{-1}) and Zn–O (430 cm^{-1}) (Kuśtrowski et al. 2005).

Thermogravimetric analysis performed on the 0.5 Zn/Mg catalyst, fresh and post-reaction, showed similar profiles and similar total mass losses (approximately 15%) (Fig. 12c). The observed peaks most probably correspond to adsorbed water. It is well known that this type of materials has the property of adsorbing water and a certain "memory effect" produced during their rehydration (Angelescu et al. 2008; Kwon et al. 2020). No significant mass loss is observed in the post-reaction catalyst that would have been associated with the total oxidation of carbonaceous species. These results agree with those obtained by FTIR.

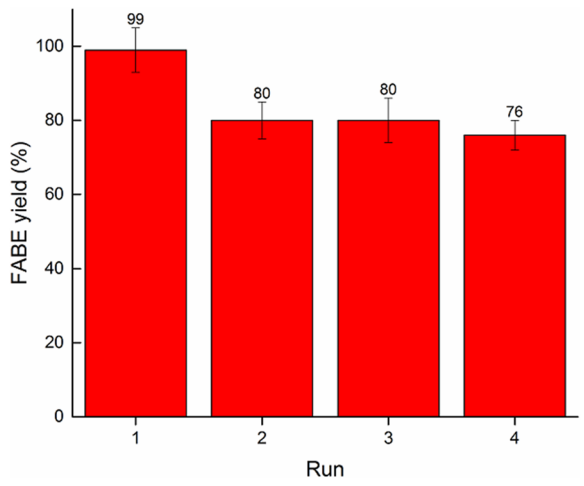

Fig. 11 Recycling test of catalyst 0.5 Zn/Mg in the transesterification of castor oil with butanol

Conclusions

All the catalysts prepared and evaluated in this work demonstrated being active in the studied reactions.

Among the prepared catalysts, the 1.5 Zn/Mg was the one with the highest surface area, with the consequent higher density of basic sites, attributed to the segregation of a magnesium aluminium hydroxide hydrate phase. These characteristics gave rise to a catalyst having a high performance in the transesterification of soybean oil and castor oil, with both methanol and butanol.

An especially remarkable result was obtained in the transesterification of castor oil with butanol. All the catalysts exhibited excellent results, with FABE yields higher than 94% and FABE selectivities of approximately 100%. The catalysts presented good performance in the transesterification of low-quality oil with a high degree of FFA, such as castor oil.

The prepared catalysts are an efficient alternative, considering that castor oil is a nonedible and renewable source, representing a cleaner approach to the production of biodiesel. In addition, butanol is an alcohol that can be obtained from renewable sources.

For this reaction, the reuse was tested, maintaining high FABE (fatty acid butyl esters) yields after four cycles.

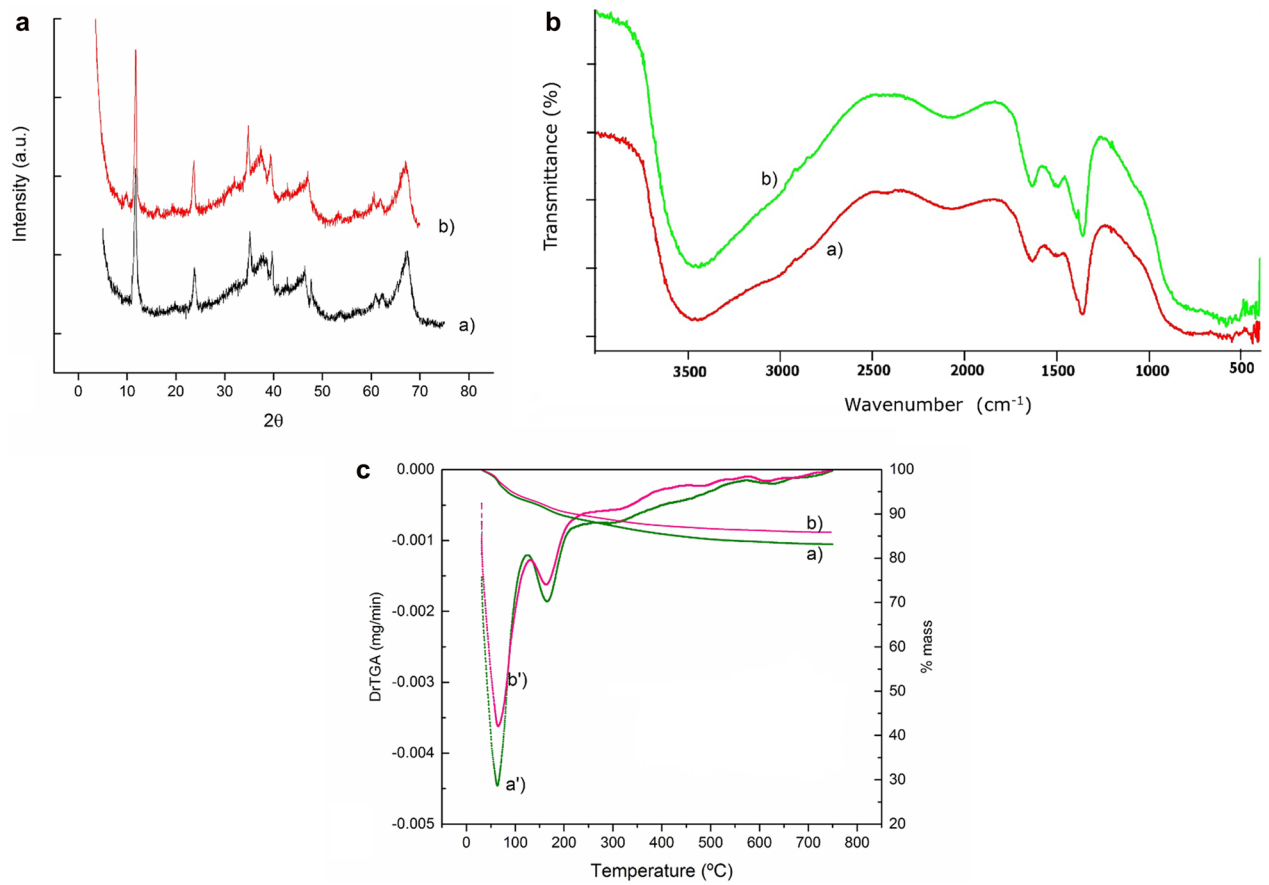

Fig. 12 **a** XRD spectra; **b** FTIR spectra and **c** thermogravimetric analysis for 0.5 Zn/Mg catalyst, a) fresh and b) after 4 reaction cycles

Additional file

Additional file 1. Additional figures.

Abbreviations

XRD: X-ray diffraction; SEM: scanning electron microscopy; EDS: energy dispersive X-ray spectroscopy; FABE: fatty acid butyl esters; FFA: free fatty acids; BET: Brunauer–Emmett–Teller; FTIR: Fourier transform infrared spectroscopy; GC: gas chromatography; EN: European Standard; ASTM: American Society of Testing Materials; FAME: fatty acid methyl ester; AAS: atomic absorption spectroscopy; JCPDS: Joint Committee on Powder Diffraction Standards.

Acknowledgements

The authors gratefully acknowledge Universidad Nacional de La Plata, Agencia Nacional de Promoción Científica y Tecnológica, and Comisión de Investigaciones Científicas de la Provincia de Buenos Aires for the financial support. The authors also acknowledge the technicians working in the Centro de Investigación y Desarrollo en Ciencias Aplicadas "Dr. Jorge J. Ronco" who performed the analyses.

Authors' contributions

MBN carried out the synthesis of the different catalysts, performed the transesterification reaction, with the previous set-up of the catalytic system, and collaborated in the analysis of the obtained results. MBN also drafted the work. JFR collaborated in the data interpretation, and also with the writing and revision of the draft. IDL performed the CO_2-adsorption experiments, and contributed to the analysis of different characterization results. IDL also contributed with the revision of the draft. MLC is the project director who provided the funds for the realization of this work. MLC also contributed to the data interpretation and the revision of the draft. All authors read and approved the final manuscript.

Funding

This work was supported by the Agencia Nacional de Promoción Científica y Tecnológica (Argentina) (PICT 2015 No 0737), the Universidad Nacional de La Plata (Argentina) (Projects X700 and X7802) and the Comisión de Investigaciones Científicas de la Provincia de Buenos Aires (CICPBA) (Argentina).

Availability of data and materials

All data generated or analyzed during this study are included in this published article and its additional files.

Ethics approval and consent to participate

Not applicable.

Consent for publication

Not applicable.

Competing interests

The authors declare that they have no competing interests.

Received: 28 October 2019 Accepted: 30 December 2019
Published online: 08 January 2020

References

Abdullah B, Muhammad S, Shokravi Z, Ismail S, Kassim K, Mahmood A, Aziz M (2019) Fourth generation biofuel: a review on risks and mitigation strategies. Renew Sustain Energy Rev 107:37–50. https://doi.org/10.1016/j.rser.2019.02.018

Adeniyi G, Ighalo J, Adeoye S, Onifade V (2019) Modelling and optimisation of biodiesel production from *Euphorbia lathyris* using ASPEN Hysys. SN Appl Sci 1:1452. https://doi.org/10.1007/s42452-019-1522-0

Alaei S, Haghighi M, Toghiani J, Vahid B (2018) Magnetic and reusable MgO/$MgFe_2O_4$ nanocatalyst for biodiesel production from sunflower oil: Influence of fuel ratio in combustion synthesis on catalytic properties and performance. Ind Crops Prod 117:322–332. https://doi.org/10.1016/j.indcrop.2018.03.015

Angelescu E, Pavel O, Birjega R, Florea M, Zavoianu R (2008) The impact of the "memory effect" on the catalytic activity of Mg/Al; Mg, Zn/Al; Mg/Al, Ga hydrotalcite-like compounds used as catalysts for cycloxene epoxidation. Appl Catal A 341(2008):50–57. https://doi.org/10.1016/j.apcata.2007.12.022

ASTM D6584. Standard test method for determination of free and total glycerin in B-100 biodiesel methyl esters by gas chromatography

Bagabas A, Alshammari A, Aboud M, Kosslick H (2013) Room-temperature synthesis of zinc oxide nanoparticles in different media and their application in cyanide photodegradation. Nanoscale Res Lett 8:516–525. https://doi.org/10.1186/1556-276x-8-516

Baskar G, Soumiya S (2016) Production of biodiesel from castor oil using iron (II) doped zinc oxide nanocatalyst. Renewable Energy 98:101–107. https://doi.org/10.1016/j.renene.2016.02.068

Boonyuen S, Smith S, Malaithong M, Prokaew A, Cherdhirunkorn B, Luengnaruemitchai A (2018) Biodiesel production by a renewable catalyst from calcined *Turbo jourdani* (Gastropoda: Turbinidae) Shells. J Cleaner Prod 177:925–929. https://doi.org/10.1016/j.jclepro.2017.10.137

Borges M, Díaz L (2012) Recent developments on heterogeneous catalysts for biodiesel production by oil esterification and transesterification reactions: a review. Renew Sustain Energy Rev 16:839–2849. https://doi.org/10.1016/j.rser.2012.01.071

Chuah L, Klemêš J, Yusup S, Bokhari A, Akbar M (2017) A review of cleaner intensification technologies in biodiesel production. J Clean Prod 146:181–193. https://doi.org/10.1016/j.jclepro.2016.05.017

Chuayplod P, Trakarnpruk W (2009) Transesterification of rice bran oil with methanol catalyzed by Mg(Al)La hydrotalcites and metal/MgAl oxides. Ind Eng Chem Res 48:4177–4183. https://doi.org/10.1021/ie8005947

Conceição M, Candeia R, Silva F, Bezerra A, Fernandes V Jr, Souza A (2007) Thermoanalytical characterization of castor oil biodiesel. Renew Sustain Energy Rev 11:964–975. https://doi.org/10.1016/j.rser.2005.10.001

da Silva Filho S, Carvalho Miranda A, Farias Silva T, Araújo Calarge F, Rodrigues de Souza R, Curvelo Santana J, Tambourgi E (2018) Environmental and techno-economic considerations on biodiesel production from waste frying oil in Sao Paulo city. J Clean Prod 183:1034–1042. https://doi.org/10.1016/j.jclepro.2018.02.199

Elango R, Sathiasivan K, Muthukumaran C, Thangavelu V, Rajesh M, Tamilarasan K (2019) Transesterification of castor oil for biodiesel production: process optimization and characterization. Microchem J 145:1162–1168. https://doi.org/10.1016/j.microc.2018.12.039

EN 14105. Fat and oil derivatives—Fatty Acid Methyl Esters (FAME)—Determination of free and total glycerol and mono-, di-, tri-glyceride content

Hájek M, Skopal F, Vávra A, Kocík J (2017) Transesterification of rapeseed oil by butanol and separation of butyl ester. J Clean Prod 1:28–33. https://doi.org/10.1016/j.jclepro.2016.07.007

Hoekman S, Broch A, Robbins C, Ceniceros E, Natarajan M (2012) Review of biodiesel composition, properties and specification. Renew Sustain Energy Rev 16:143–169. https://doi.org/10.1016/j.rser.2011.07.143

Issariyakul T, Dalai A (2014) Biodiesel from vegetable oils. Renew Sustain Energy Rev 31:446–471. https://doi.org/10.1016/j.rser.2013.11.001

Keera S, El Sabagh S, Taman A (2018) Castor oil biodiesel production and optimization. Egypt J Petrol 27:979–984. https://doi.org/10.1016/j.ejpe.2018.02.007

Knothe G, Razón L (2017) Biodiesel fuels. Prog Energy Combust Sci 58:36–59. https://doi.org/10.1016/j.pecs.2016.08.001

Koh MY, Mohd Ghazi TI (2011) A review of biodiesel production from *Jatropha curcas* L. oil. Renew Sustain Energy Rev 15:2240–2251. https://doi.org/10.1016/j.rser.2011.02.013

Kolesinska B, Fraczyk J, Binczarski M, Modelska M, Berlowska J, Dziugan P, Antolak H (2019) Butanol synthesis routes for biofuel production: trends and perspectives. Materials 12:350. https://doi.org/10.3390/ma12030350

Kumar M, Gayen K (2011) Developments in biobutanol production: new insights. Appl Energy 88:1999–2012. https://doi.org/10.1016/j.apenergy.2010.12.055

Kuśtrowski P, Sułkowska D, Chmielarz L, Rafalska-Łasocha A, Dudek B, Dziembaj R (2005) Influence of thermal treatment conditions on the activity of hydrotalcite-derived Mg–Al oxides in the aldol condensation of acetone. Microporous Mesoporous Mater 78:11–22

Kwon D, Kang Y, An S, Yang I, Jung J (2019) Tuning the base properties of Mg–Al hydrotalcite catalysts using their memory effect. J Energy Chem 46(2020):229–236. https://doi.org/10.1016/j.jechem.2019.11.013

Lee A, Wilson K (2015) Recent developments in heterogeneous catalysis for the sustainable production of biodiesel. Catal Today 242:3–18. https://doi.org/10.1016/j.cattod.2014.03.072

Lee H, Yunus R, Juan J, Taufiq-Yap Y (2011) Process optimization design for jatropha-based biodiesel production using response surface methodology. Fuel Process Technol 92:2420–2428. https://doi.org/10.1016/j.fuproc.2011.08.018

Lee H, Taufiq-Yap Y, Hussein M, Yunus R (2013) Transesterification of jatropha oil with methanol over MgZn mixed metal oxide catalysts. Energy 49:12–18. https://doi.org/10.1016/j.energy.2012.09.053

Lin CY, Lin HA, Hung LB (2006) Fuel structure and properties of biodiesel produced by the peroxidation process. Fuel 85:1743–1749. https://doi.org/10.1016/j.fuel.2006.03.010

Mahdavi V, Monajemi A (2014) Optimization of operational conditions for biodiesel production from cottonseed oil on CaO–MgO/Al2O3 solid base catalysts. J Taiwan Inst Chem Eng 45:2286–2292. https://doi.org/10.1016/j.jtice.2014.04.020

Margellou A, Koutsouki A, Petrakis D, Vaimakisa T, Manosb G, Kontominasa M, Pomonis P (2018) Enhanced production of biodiesel over MgO catalysts synthesized in the presence of Poly-Vinyl-Alcohol (PVA). Ind Crops Prod 114:146–153. https://doi.org/10.3390/ma12030350

Meneghetti S, Meneghetti M, Wolf C, Silva E, Lima G, de Lira Silva L, Serra T, Cauduro F, de Oliveira L (2006) Biodiesel from castor oil: a comparison of ethanolysis versus methanolysis. Energy Fuels 20:2262–2265. https://doi.org/10.1021/ef060118m

Meneghetti SM, Meneghetti MR, Serra TM, Barbosa DC, Wolf CR (2007) Biodiesel production from vegetable oil mixtures: cottonseed, soybean, and castor oils. Energy Fuels 21:3746–3747. https://doi.org/10.1021/ef070039q

Navas M, Lick I, Bolla P, Casella M, Ruggera J (2018) Transesterification of soybean and castor oil with methanol and butanol using heterogeneous basic catalysts to obtain biodiesel. Chem Eng Sci 187:444–454. https://doi.org/10.1016/j.ces.2018.04.068

Neimark A, Sing K, Thommes M (2008) Characterization of solid catalysts. In: Ertl G, Knözinger H, Schüth F, Weitkamp J (eds) Handbook of heterogeneous catalysis, vol 2. Wiley, New York, p 72

Ngamcharussrivichai C, Totarat P, Bunyakiat K (2008) Ca and Zn mixed oxide as a heterogeneous base catalyst for transesterification of palm kernel oil. Appl Catal A 341:77–85. https://doi.org/10.1016/j.apcata.2008.02.020

Olutoye M, Hameed B (2013) Production of biodiesel fuel by transesterification of different vegetable oils with methanol using Al_2O_3 modified MgZnO catalyst. Bioresour Technol 132:103–108. https://doi.org/10.1016/j.biortech.2012.12.171

Pan H, Li H, Zhang H, Wang A, Jin D, Yan S (2018) Effective production of biodiesel from non-edible oil using facile synthesis of imidazolium salts-based Brønsted–Lewis solid acid and co-solvent. Energy Convers Manage 166:534–544

Pasupulety N, Rempel G, Ng F (2015) Studies on Mg-Zn mixed oxide catalyst for biodiesel production. Appl Catal A 489:77–85. https://doi.org/10.1016/j.apcata.2014.10.015

Rahman W, Fatima A, Anwer A, Athar M, Khan M, Khan N, Halder G (2019) Biodiesel synthesis from eucalyptus oil by utilizing waste egg shell-derived calcium based metal oxide catalyst. Process Saf Environ Prot 122:313–319. https://doi.org/10.1016/j.psep.2018.12.015

Rubio-Caballero J, Santamaría-González J, Mérida-Robles J, Moreno-Tost R, Jiménez-López A, Maireles-Torres P (2009) Calcium zincate as precursor of active catalysts for biodiesel production under mild conditions. Appl Catal B 91:339–346. https://doi.org/10.1016/j.apcatb.2009.05.041

Sánchez M, Navas M, Ruggera J, Casella M, Aracil J, Martínez M (2014) Biodiesel production optimization using γ-Al_2O_3. Energy 73:661–669. https://doi.org/10.1016/j.energy.2014.06.067

Shan R, Lu L, Shia Y, Yuan H, Shie J (2018) Catalysts from renewable resources for biodiesel production. Energy Convers Manag 178:277–289. https://doi.org/10.1016/j.enconman.2018

Sharma Y, Singh B, Korstad J (2011) Latest developments on application of heterogenous basic catalysts for an efficient and eco-friendly synthesis of biodiesel: a review. Fuel 90:1309–1324. https://doi.org/10.1016/j.fuel.2010.10.015

Steen EJ, Chan R, Prasad N, Myers S, Petzold C, Redding A, Ouellet M, Keasling JD (2008) Metabolic engineering of Saccharomyces cerevisiae for the production of n-butanol. Microb Cell Fact 7:1–8. https://doi.org/10.1186/1475-2859-7-36

Sun S, Li X (2016) Functional ionic liquids catalyzed the esterification of ricinoleic acid with methanol to prepare biodiesel: optimization by response surface methodology. J Am Oil Chem Soc 93:757–764. https://doi.org/10.1007/s11746-016-2826-5

Sun S, Guo J, Duan X (2019) Biodiesel preparation from Phoenix tree seed oil using ethanol as acyl acceptor. Ind Crops Prod 137:270–275. https://doi.org/10.1016/j.indcrop.2019.05.035

Thommes M, Kaneko K, Neimark A, Olivier J, Rodriguez-Reinoso F, Rouquerol J, Sing K (2015) Physisorption of gases, with special reference to the evaluation of surface area and pore size distribution (IUPAC Technical Report). Pure Applied Chemistry 87(9–10):1051–1069

Ullah F, Dong L, Bano A, Peng Q, Huang J (2016) Current advances in catalysis toward sustainable biodiesel production. J Energy Inst 89:282–292. https://doi.org/10.1016/j.joei.2015.01.018

Veiga P, Veloso C, Henriques C (2016) Synthesis of Zn, La-catalysts for biodiesel production from edible and acid soybean oil. Renew Energy 99:543–552. https://doi.org/10.1016/j.renene.2016.07.035

Wang P, Sun S (2016) Enhanced enzymatic preparation of biodiesel using ricinoleic acid as acyl donor: optimization using response surface methodology. J Oleo Sci 65(9):785–795. https://doi.org/10.5650/jos.ess16052

Xi Y, Davis RJ (2011) Nanocrystalline MgO catalysts for the Henry reaction of benzaldehyde and nitromethane. Renew Sust Energy Rev J Mol Catal A 341:22–27. https://doi.org/10.1016/j.molcata.2011.03.018

Yan S, Salley S, Ng K (2009) Simultaneous transesterification and esterification of unrefined or waste oils over ZnO–La_2O_3 catalysts. Appl Catal A 353:203–212. https://doi.org/10.1016/j.apcata.2008.10.053

Yan F, Yuan Z, Lu P, Luo W, Yang L, Deng L (2011) FeZn double-metal cyanide complexes catalyzed biodiesel production from high-acid-value oil. Renew Energy 36:2026–2031. https://doi.org/10.1016/j.renene.2010.10.032

Zhang Q, Li H, Yang S (2018a) Facile and low-cost synthesis of mesoporous Ti–Mo Bi-metal oxide catalysts for biodiesel production from esterification of free fatty acids in jatropha curcas crude oil. J Oleo Sci 67(5):579–588. https://doi.org/10.5650/jos.ess17231

Zhang Q, Wei F, Ma P, Zhang Y, Wei F, Chen F (2018b) Mesoporous Al–Mo oxides as an effective and stable catalyst for the synthesis of biodiesel from the esterification of free-fatty acids in non-edible oils. Waste Biomass Valor 9:911–918. https://doi.org/10.1007/s12649-017-9865-5

Publisher's Note